LIMNOLOGY and OCEANOGRAPHY

Multiscale effects of wind-induced hydrodynamics on lake plankton distribution

William Gary Sprules ,[1]* Hélène Cyr ,[2] Charles W. Menza [1,a]
[1]Department of Biology, University of Toronto Mississauga, Mississauga, Ontario, Canada
[2]Department of Ecology & Evolutionary Biology, Ramsay Wright Zoological Labs, St. George Campus, University of Toronto, Toronto, Ontario, Canada

Abstract

In this study, we used a combination of high-intensity sampling technologies, and a 3D hydrodynamic model of a medium-sized lake in southern Ontario, Canada to investigate physical–biological relationships at spatial scales from 100 m to 6 km and temporal scales from hours to months. At the scale of the whole study basin, we predicted that stronger winds would lead to higher zooplankton biomass downwind relative to upwind. The hydrodynamic model suggests rapid downwind displacement of progressively deeper surface mixed layers with increasing winds, and we found a statistically higher downwind biomass of small-bodied zooplankton on windy days, but not large zooplankton. At a fine spatial scale (hundreds of meters), we predicted that zooplankton patchiness would decrease with increasing wind mixing of the upper water column and confirmed this for small-bodied but not large-bodied zooplankton. At this fine-scale cross-correlations of zooplankton biomass with water temperature and chlorophyll fluorescence suggested that zooplankton are not simply moved passively by water masses. We also found a clear change in the cross-correlation between large- and small-bodied zooplankton biomass, with out-of-phase spatial distributions during calm periods becoming in-phase with increasing winds. Overall these results indicate that the response of zooplankton to wind-driven physical forces is strongly dependent on an interaction between their body size, which determines their swimming speed and capacity to position themselves vertically in the water column, and the spatial scale and intensity of the wind-generated physical forces. We discuss the implications for food web interactions.

The effects of wind forces across the surface of thermally stratified lakes are generally well understood (Wüest and Lorke 2003; Monismith and MacIntyre 2009). These

*Correspondence: gary.sprules@utoronto.ca

Additional Supporting Information may be found in the online version of this article.

[a]Present address: National Centers for Coastal Ocean Science, NOAA National Ocean Service, Silver Spring, Maryland

Author Contribution Statement: CWM - during his MSc thesis research he conceived the basic design of our field study and collected all the zooplankton field data. He also helped with organizing and writing the manuscript. HC - collected the water temperature and meteorological data and implemented the ELCOM modelling. She also helped with organizing and writing the manuscript. WGS - supervised and helped design the MSc research, processed the zooplankton data, and helped with organizing and writing the manuscript.

physical forces will affect the spatial distribution of algae and zooplankton in the water column as a function of their motility, evolved responses to physical and chemical gradients such as light and temperature, diel vertical migration, their need to locate resources such as nutrients and light for algae and prey for zooplankton, and to avoid predators (Malone and McQueen 1983; Prairie et al. 2012). Such spatial patterns have been documented in a variety of studies that generally show more passive species to be entrained downwind by near-surface water currents (George and Edwards 1976; Cyr 2017) and sometimes to be returned upwind by reverse currents developing above the metalimnion (George and Heaney 1978). Models show that only planktonic organisms able to maintain their vertical position in the water column will be concentrated downwind (Verhagen 1994).

In a recent review of how physical dynamics in lakes and oceans can affect plankton distributions and interactions, Prairie et al. (2012) pointed out that most studies are conducted over a narrow range of spatial scales, yet biophysical interactions occur at multiple scales. The objective of our study was

to evaluate current hypotheses about the effects of winds of varying strength on the fluid environment of a moderately large inland lake and associated effects on plankton distributions across a wide range of spatial and temporal scales. We used a combination of high-intensity sampling technologies for plankton (towed optical plankton counter and fluorometer) and water temperature (towed thermistor, thermistor strings), in combination with a 3D hydrodynamic model, to investigate physical–biological relationships from spatial scales of hundreds of meter up to 6 km and temporal scales from hours to months.

Our conceptual framework for the study is outlined in Fig. 1. We assume that the dominant physical forces controlling fine- and coarse-scaled spatial distributions of zooplankton range from weak stratification in the upper water column under light winds to full upwellings and full epilimnetic mixing with strong winds. We also assume that in general small zooplankton are transported more passively than large zooplankton and their distribution would thus be more closely related to physical processes. We use high-resolution plankton data collected under these different states of the water column and over a wide range of wind conditions to answer three questions about zooplankton distribution at different spatial scales: (1) At a basin scale, do zooplankton accumulate downwind on windy days, and do small zooplankton accumulate more than large zooplankton? (2) At a fine spatial scale, does zooplankton patchiness decrease with increasing winds, and is this relationship the same for small and large zooplankton? (3) At a fine scale, do spatial correlations between components of the plankton community change with increasing wind? We report evidence of systematic changes in both fine- and basin-scale patterns of zooplankton distribution with increasing wind forcing and discuss the implications of these findings for trophic interactions in planktonic communities.

Materials

Study site

Lake Opeongo is a dimictic oligo-mesotrophic lake located on the Precambrian Shield in Algonquin Park, Ontario, Canada (45°42′N, 78°22′W). Our research was conducted during thermal stratification in the South Arm (surface area 22.1 km^2, maximum depth 50 m, mean depth 14.6 m; Fig. 2), within the central basin that is oriented roughly parallel to prevailing northwesterly winds with a maximum effective fetch of ~ 6 km. The Ontario Ministry of Natural Resources and Forestry (OMNRF) produced a high-resolution bathymetric map of the whole lake and maintains two thermistor strings and a weather station on South Arm during the ice-off season, which allow calibration and validation of hydrodynamic models. The Estuary, Lake, and Coastal Ocean 3D hydrodynamic Model (3D-ELCOM) has proven particularly successful at reproducing the thermal structure measured in
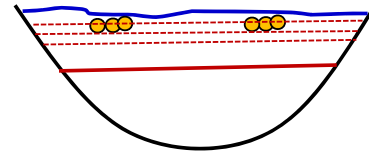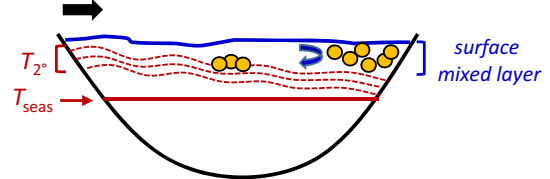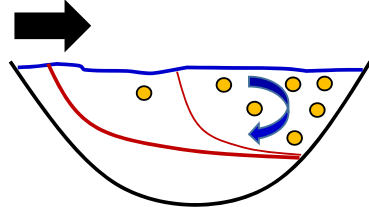

Fig. 1. Conceptual model showing changes in stratification with variations in wind speed and mixing that are expected to affect the distribution of zooplankton in lakes. Solid red lines indicate the seasonal thermocline (T_{seas}), dotted red lines are isotherms in the secondary thermocline ($T_{2°}$), the layer above the secondary thermocline is the surface mixed layer and circles represent zooplankton. Black arrows indicate wind direction and relative strength. (**a**) On calm sunny days, and during extended periods of light winds, stratification in the form of diurnal or secondary thermoclines develops close to the surface and the surface mixed layer is shallow. Zooplankton can position themselves vertically in the water column in response to light, algal prey and predators. We predict high fine-scale spatial variability of zooplankton with no basin-scale difference in biomass across the basin. (**b**) Weak to moderate steady winds displace the diurnal or secondary thermoclines and concentrate surface plankton, particularly small zooplankton (weak swimmers) at the downwind end of the lake basin. We predict high spatial variability for both small and large zooplankton and a positive upwind to downwind gradient in zooplankton biomass, particularly for small zooplankton. (**c**) Very windy days, with full upwelling of the seasonal thermocline concentrate epilimnetic zooplankton downwind and upwell metalimnetic water with lower zooplankton concentrations at the upwind end of the lake basin. We predict low fine-scale spatial variability due to strong surface mixing and a large basin-scale gradient in zooplankton biomass.

South Arm, both offshore (Cyr 2017) and nearshore (Cyr 2016).

Field transect data

Plankton and water temperature data were collected 1–5 times per day on 21 different days from early to late thermal stratification (June, July, and September 2001, Table 1; Menza 2003). Sampling was conducted during daylight
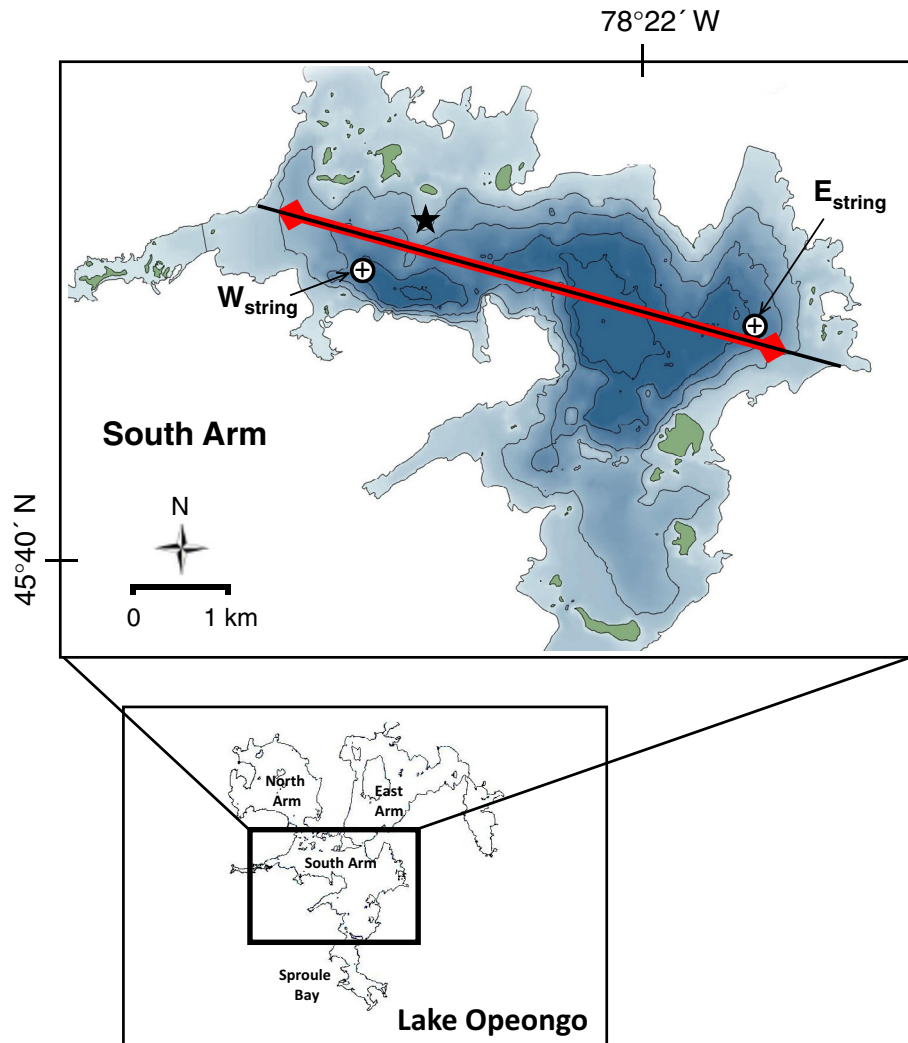
Fig. 2. Map of South Arm in Lake Opeongo, Ontario, Canada, showing location of the OPC standard transect (thick red line), and of the transect used for ELCOM outputs (black line extending beyond the OPC transect). Star is the weather station; crossed circles are vertical thermistor stings (W_{string}, E_{string}). Bathymetric contours at 10-m interval.

hours (09 : 25–17 : 30, Table 1) to minimize the effect of zooplankton diel vertical migration which in this lake comprises the typical crepuscular movements into and out of the epilimnion by strong migrators such as some copepod and *Daphnia* species. Daytime vertical migration of zooplankton in and out of the upper water column where we sampled is typically negligible (L.E. Barth and W.G. Sprules unpubl. data).

Electronic sensors for measuring water temperature, fluorescence, and zooplankton biomass were attached to rigid vertical poles fixed to either side of a motorboat and towed at a fixed depth of 2.5 m. The poles were located near the bow to avoid disturbances caused by the motor's propeller. Continuous measurements were taken along 52 transects aligned with the long axis of South Arm (Fig. 2) under a range of wind speeds and directions. Transect lengths ranged from 2.9 to 5.0 km (mean = 4.3 km; average time to complete ~ 50 min). There were

modest variations in the precise track sampled, so we averaged the position of all measured transects to establish a standard transect with distance 0 upwind and distance 1 downwind (thick red line in Fig. 2). The individual transect routes were projected (north–south projection) on to the standard transect for analysis.

Water flow through the instruments was measured with an electronic flowmeter (General Oceanics) and water temperature recorded with a conductivity–temperature–depth probe (Ocean Sensors). A fluorometer (AquaTracka III, Chelsea Technologies) was used to measure chlorophyll *a* (Chl *a*) fluorescence (excitation 430 nm, emission 685 nm, accuracy $\pm 3\%$) and was empirically calibrated to Chl *a* concentration ($\mu g\,L^{-1}$; M. Charlton, Environment Canada, Burlington ON, pers. comm.). Near surface fluorescence is a poor indicator of algal biomass due to photoprotective quenching (Cyr 2017). In Lake Opeongo Chl *a* concentration is uniform through the epilimnion (Cyr 2017), so fine-scale changes in fluorescence

Table 1. Sampling dates and starting times of OPC transects, with wind and physical condition of the lake basin during sampling. n_{OPC} is the number of OPC transects sampled on each day. $T/4$ is one quarter of the seiche period (see text for details). For each sampling date, we list mean Wind Force and mean Lake Number, both calculated over $T/4$ h prior to sampling; ranges with increasing or decreasing values reflect trends in conditions when multiple samples per day were taken. Predominant winds are westerly.

Date	n_{OPC}	Starting times	$T/4$ (h)	Wind Force, prior $T/4$ h (m s^{-1})	Lake Number, prior T/4 h
06 Jun	3	10 : 43–15 : 52	10.9	2.1	8–6
07 Jun	4	10 : 02–13 : 18	10.9	1.4–1.5	29–19
18 Jun	1	10 : 29	8.0	3.6	2
19 Jun	1	9 : 53	8.0	2.0	1
20 Jun	1	9 : 34	8.0	2.7	9
22 Jun	3	10 : 02–12 : 22	8.0	4.6–3.6*	4–5
23 Jun	3	10 : 06–14 : 41	8.0	2.8–2.1	5
24 Jun	2	9 : 25–10 : 26	8.0	1.6–1.5	22–30
04 Jul	1	17 : 10	9.8	1.9	28
05 Jul	2	11 : 49–14 : 32	9.8	5.7–6.4	2–1
06 Jul	1	9 : 41	9.8	4.5	4
07 Jul	1	17 : 02	9.8	3.1	3
08 Jul	2	13 : 14–14 : 14	9.8	1.5–1.7	33–25
09 Jul	4	10 : 20–13 : 27	9.8	2.1–1.6	26–50
10 Jul	5	11 : 15–15 : 22	9.8	1.2–1.7	24–12
13 Jul	4	11 : 55–14 : 25	8.9	4.1–4.2	4–3
14 Jul	3	10 : 33–12 : 14	8.9	2.8–2.9	5–4
17 Jul	3	9 : 31–15 : 32	8.9	1.4–0.6	62–179
19 Jul	5	9 : 50–15 : 15	8.9	0.7–2.6*	141–15
22 Sept	2	16 : 15–17 : 17	14.1	2.4–2.6	18–17
23 Sept	1	14 : 01	14.1	1.2	33

*Easterly winds.

along the transects likely reflect vertical movement of algae that fluoresce differently past our fixed sampling depth (2.5 m). We interpret fluorescence peaks along these transects as upward movement of deeper epilimnetic water, and fluorescence troughs as downward movement of surface water.

Zooplankton were sampled with an Optical Plankton Counter (Model OPC-1T, Focal Technologies Inc.) that sized and counted particles from 250 µm to 2 cm in equivalent circular diameter (ECD). A clear acrylic plate was inserted into the OPC sampling tunnel to reduce the volume of water passing the sensors and thus reduce coincident particle counts (Sprules et al. 1998). Zooplankton were divided into two size ranges—small zooplankton (≤ 507 µm ECD roughly including bosminid cladocerans, copepod nauplii, early copepodid stages, juvenile daphnids, *Ceriodaphnia*, *Diaphanosoma*, and *Holopedium*) and large zooplankton (> 507 µm ECD including adult copepods and daphnids, *Leptodora*, and *Polyphemus*). ECDs were converted to mass by a using an ellipsoid model with long axis equal to the ECD and short axis equal to ECD/1.8 (Sprules et al. 1998; Finlay et al. 2007) and total biomass concentrations expressed as µg L^{-1} (wet mass). The boat was driven as close as possible to a steady velocity of 1.5 m s^{-1} which, in combination with the sampling rate of 1 Hz, gave a

linear spatial resolution of ~ 1.5 m. These biomass data contained a lot of high-frequency noise that is not unusual for OPC observations. We determined the most appropriate filter with which to minimize this noise using spectral analysis for large- and small-bodied zooplankton from a subset of transects sampled at different times of the year (06 June, 08 July, 19 July). These spectra showed white noise down to a frequency of ~ 0.015 (= 1/67 observations), so we ran a moving average with a window of 67 observations (~ 100 m) over all zooplankton data, and these filtered data were used in all subsequent analyses.

Our basic transect data thus comprise continuous measurements of four variables (chlorophyll fluorescence, water temperature, and large- and small-bodied zooplankton biomass) along a 2.5-m-deep linear transect. An independent observation is a single traverse of the transect and we collected 52 such observations during our field season.

Measures of spatial distribution

We calculated three indices of zooplankton distribution at different spatial scales. Basin-scale patterns were expressed as a Relative Biomass Index (RBI; Menza 2003)—the ordinary least squares slope of a straight line fitted to their biomass

vs. standardized transect distance relationship (Supporting Information Fig. S1A). Although boat travel along the transect was independent of wind direction at sampling time, we oriented the data for each transect observation from upwind to downwind based on measured wind direction. Positive values of RBI indicate higher biomass at the downwind end relative to the upwind end of the basin and could result from accumulation of biomass downwind or from decline of biomass upwind (Fig. 1c). Negative values indicate the reverse.

Fine-scale spatial variability was quantified as the coefficient of variation (CV) of the detrended transect data—the standard deviation of all residuals from the straight line used to calculate RBI divided by the transect mean (Supporting Information Fig. S1B). This is a standardized measure of point-to-point spatial variability in the 100-m-filtered data along the transect.

We also measured how strongly biomasses of the two zooplankton size groups along the transects were related to one another, or to temperature or fluorescence. This was done by calculating cross-correlations (X-corr) after linearly detrending the transect data to remove basin-scale patterns (Supporting Information Fig. S1C). High positive/negative X-corr indicates two variables (e.g., small zooplankton biomass and temperature) showed a similar/opposite spatial response to fine-scale biological and hydrodynamic processes whereas low X-corr indicates no spatial relationship between two transect variables.

Meteorological and water temperature instrumentation

The weather station sits 3.8 m above the lake on a small rocky island in the western part of the study basin (star in Fig. 2) and is maintained by OMNRF. The station includes a Campbell CR10X equipped with a CS500 temperature and relative humidity probe, a 05103-10 RM Young wind monitor, a Kipp & Zonen CM6B silicon pyranometer, a LI-190SZ Li-Cor PAR sensor and a Texas Electronics TE525 tipping bucket rain gauge. Meteorological data were collected at 10-min intervals from mid-May to late October.

Profiles of water temperature and the seasonal development of lake stratification were recorded using two offshore vertical thermistor chains (W_{string}, E_{string} in Fig. 2), each fitted with 10 Hobo loggers (Temp Pro H20-001, Onset; accuracy $\pm 0.2°C$) recording at 8-min interval and positioned at 1.5-m interval through the epilimnion and metalimnion (0.5–13 m), plus one thermistor in the hypolimnion (19.5 m).

Calculation of physical variables

Wind force (WF, m s^{-1}) weighs the components of measured wind speed according to their orientation with the standard transect (Menza 2003):

$$WF = \sum_{i=1}^{n} (\cos(DEV_i) \times ws_i)/n,$$

where i is a wind measurement, n is the total number of wind measurements being averaged, DEV (radians) is the deviation of each wind measurement from the standard transect

axis (285°), and ws is the wind speed (m s^{-1}). Instead of arbitrarily choosing a single time scale for analysis, we calculated the arithmetic mean of WF over increasing time scales from 1 to 24 h before sampling began, with a 1-h time step (following Holland et al. 2004). We also calculated average WF over a time scale of ¼ the seiche period ($T_{V2H1}/4$ h or $T/4$ for simplicity; Stevens and Imberger 1996). Outputs from our 3D hydrodynamic model (see below) suggest a three-layer water column, so we calculated the vertical mode 2 horizontal mode 1 (V2H1) internal seiche period using dynmodes Matlab code (Klinck 1999, accessed through https://sea-mat.github.io/sea-mat/, December 2020).

Lake Number (LN) is the ratio of the stabilizing forces of thermal stratification to the destabilizing effects of wind-induced forces, taking the observed water column stratification and lake hypsography into account, and is a useful indicator of upwelling activity of the seasonal thermocline and of mixing from this upwelling activity (Monismith and MacIntyre 2009). We used Lake Analyzer (Read et al. 2011) to calculate LN from wind data, thermal profiles measured at W_{string} and detailed lake bathymetric data provided by OMNRF. LN was averaged (geometric mean) over various time scales as for WF.

Energy dissipation ($\mathcal{E}_{calc}$) is an indicator of turbulence in the upper water column generated from wind shear and convective cooling. Following Imberger (1985) and Serra et al. (2007), we calculated wind friction velocity (u^*) and convective velocity scales (w^*), and estimated $\mathcal{E}_{calc}$ in the surface mixed layer (Supporting Information "Physical variables" section). This allowed us to calculate turbulent velocity scale (u_{turb}) in the surface mixing layer (Supporting Information "Physical variables" section), which can be compare to zooplankton swimming speed (Denman and Gargett 1983).

Hydrodynamic model

We used the 3D-ELCOM model (Hodges and Dallimore 2014) to visualize basin wide stratification and upwelling/downwelling activity in South Arm. Thermal patterns in the water column thus revealed help in interpretation of the physical forces creating observed patterns in the spatial distribution of zooplankton. The ELCOM model was set to produce outputs along the same east–west axis as the OPC standard transect (thin black line in Fig. 2). The model was set up with a 50-m horizontal grid as described by Cyr and Sprules (2022) and was calibrated and validated over the sampling period. There was very good agreement between simulated temperatures and those recorded both by the OPC and the two vertical thermistor strings (Supporting Information "Hydrodynamic model calibration" section; Table S1; Fig. S2).

Statistical methods

We treat the two physical forcing variables (Wind Force and Lake Number) as continuous variables and assessed their relationships with zooplankton spatial response variables (RBI,

Table 2. Statistics for linear regressions between several indices of zooplankton distribution and physical variables. Relationships are shown for physical forcing variables averaged over $T/4$ with the single exception of large zooplankton cross-correlation with fluorescence for which the 2 h fixed window had a higher R^2 value (see "Methods" section). Results on the left are for small zooplankton ($\leq$ 507 μm ECD), on the right for large zooplankton (> 507 μm ECD). X-corr is the r coefficient of a cross-correlation, WF is mean Wind Force and LN is geometric mean Lake number. The coefficient of determination (R^2) and the probability (p) from the regression test are shown. Results highlighted in bold are plotted in Figs. 5, 6. Relationships for large zooplankton were non-significant ($p > 0.05$), and R^2 values are not reported ($-$) in those cases.

Zoop distribution variable	Physical variable	Small zooplankton			Large zooplankton		
		Best time scale (h)	R^2	p	Best time scale (h)	R^2	p
RBI	Log$_{10}$WF	**T/4**	**0.41**	**<0.00001**	T/4	—	**>0.2**
	Log$_{10}$LN	T/4	0.23	0.0003	T/4	—	>0.4
log$_{10}$CV	log$_{10}$WF	T/4	0.14	0.002	**T/4**	—	**>0.15**
	Log$_{10}$LN	**T/4**	**0.32**	**0.00001**	T/4	—	>0.6
X-corr with temperature	Log$_{10}$WF	T/4	0.17	0.002	**T/4**	—	**0.057**
	Log$_{10}$LN	**T/4**	**0.24**	**0.0002**	T/4	—	>0.4
X-corr with fluorescence	Log$_{10}$WF	**T/4**	**0.32**	**0.00001**	2	—	**0.07**
	Log$_{10}$LN	T/4	0.27	0.00008	2	—	0.09
X-corr with large zoop	Log$_{10}$WF	**T/4**	**0.52**	**< 0.00001**			
	Log$_{10}$LN	T/4	0.49	< 0.00001			

CV, and X-corr with temperature, fluorescence and the other zooplankton group, for each size class of zooplankton) using ordinary least squares regression. Each relationship was calculated using physical variables at various time scales as described above. We selected the physical variable with the highest R^2, and since there was little difference in statistical strength between the fixed time lags vs. $T/4$ we always plotted the latter with one exception noted in Table 2 below.

Results

Physical forces in the upper water column

OPC plankton transects were sampled under a wide range of wind conditions (Table 1; Fig. 3a,b), from early stratification (06–07 June) through well-stratified summer conditions when the seasonal thermocline progressively strengthened and deepened (18 June–19 July) and a secondary thermocline developed (e.g., 17–19 July), to late stratification in the fall (22–23 September; Fig. 4; Supporting Information Fig. S3). This provides a wide range of physical conditions (Fig. 3) that could affect the spatial distribution of zooplankton in the surface layer of South Arm.

On calm sunny days with positive heat fluxes (Fig. 3e; also see Supporting Information "Detailed time series" section), the surface water becomes stratified and essentially caps the water column and preserves whatever stratification was present in the lower portion of the epilimnion (e.g. Fig. 4b; Supporting Information Fig. S3D). The ELCOM model suggests that light winds on these calm days are sufficient to tilt the secondary isotherms slightly and push the thin surface mixed layer to the downwind end of the basin. Mild winds can upwell the upwind portion of some isotherms to the lake surface

(e.g., Fig. 4a; Supporting Information Fig. S3E). Slightly stronger winds blowing for some time can tilt and energize a stratified layer (e.g., secondary thermocline, Fig. 4c,d; seasonal thermocline during early stratification; Supporting Information Fig. S3B,C). Strong winds blowing for a long enough time are expected to mix the epilimnion, tilt the seasonal thermocline and produce an upwelling at the upwind end of the lake basin (Stevens and Imberger 1996). Lake Number varied several orders of magnitude during our sampling (Fig. 3c; Supporting Information Figs. S4–S8) with brief periods of LN < 1 suggesting full upwelling to the lake surface (19 and 22 June, 05 July). However the ELCOM hydrodynamic model suggests no full (hypolimnetic) upwelling (e.g., Fig. 4f), possibly because those very windy periods were too short (< $T/4$ of 9.8 h; Supporting Information Figs. S4–S8). Instead, on windy sampling days the ELCOM model shows mixing down to the seasonal thermocline and partial upwellings from the upper portion of the metalimnion that reached the lake surface, sometimes more than halfway down the 6 km basin (e.g., Fig. 4e–h; Supporting Information Fig. S3A,B). These partial (metalimnetic) upwellings occur at LN < 10 and are common in Lake Opeongo (51% of LN values from 01 June to 23 September, Fig. 3c). Partial upwellings effectively displace the whole epilimnetic water mass downwind for a few hours to days depending on the winds.

Statistical trends in zooplankton spatial patterns

In this section we first show how the spatial distributions of zooplankton are statistically related to the physical variables (Figs. 5, 6), and in the following section use a subset of our transects to illustrate how thermal stratification and physical
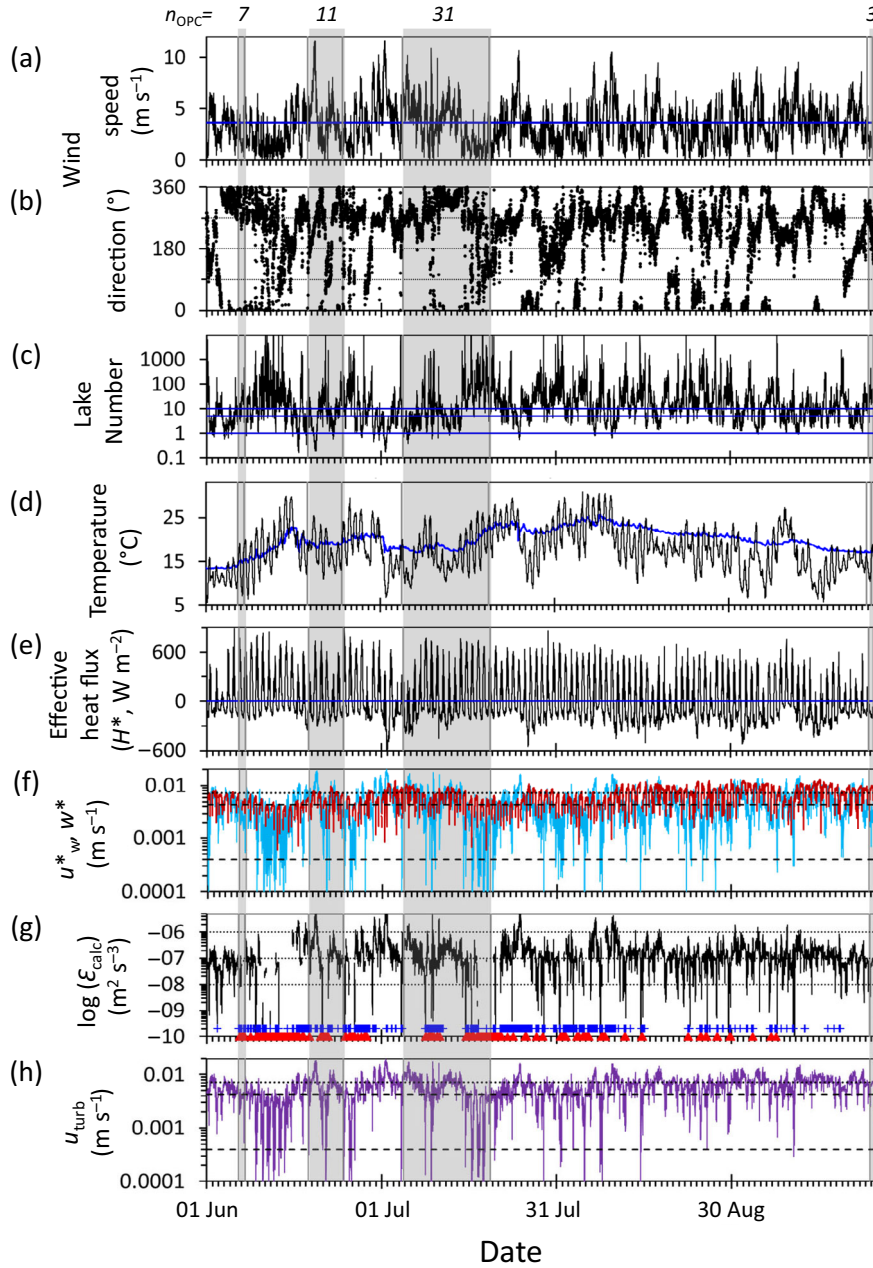
Fig. 3. Time series of atmospheric forcing, heat flux and lake conditions over the summer 2001 in the South Arm of Lake Opeongo. Sampling periods are highlighted with shading and number of OPC transects sampled in each period (n_{OPC}) is shown at the top. (**a,b**) Wind speed and direction. Horizontal reference lines are mean wind speed (3.6 m s^{-1}) and cardinal directions in (**a**) and (**b**), respectively. (**c**) Lake Number. Horizontal reference lines indicate LN = 1, 5 and 10; LN < 1 suggests a full upwelling, LN between 1 and 10 a partial upwelling, and LN > 10 calm conditions without upwelling. (**d**) Air (black line) and surface water (thick blue line) temperatures. (**e**) Effective heat flux (H^*). (**f**) Velocity scales attributed to wind shear (u^*, light blue) and to thermal convection (w^*, red). Lower dashed reference lines: range of typical swimming speeds of zooplankton species found in Lake Opeongo (0.4–4.3 mm s^{-1}; Supporting Information "Zooplankton swimming speeds" section), upper dotted reference line: typical swimming speed of *Epischura lacustris*, a large predatory copepod also found in Lake Opeongo. (**g**) Calculated rate of energy dissipation ($\mathcal{E}_{calc}$) in the surface mixed layer. Symbols at the bottom of the graph highlight periods when OPC transects were partially (blue crosses) or fully (red triangles) located in the stratified portion of the epilimnion, below the surface mixed layer (Supporting Information Fig. S2). $\mathcal{E}_{calc}$ was not plotted when the OPC transect sampling depth was below the surface mixed layer (red triangles). Reference lines indicate high ($\mathcal{E} > 10^{-6}$ m^2 s^{-3}), moderate ($\mathcal{E} \sim 10^{-7}$ m^2 s^{-3}) and weak ($\mathcal{E} \leq 10^{-8}$ m^2 s^{-3}) turbulence (Supporting Information "Physical variables" section). (**h**) Velocity scales calculated from $\mathcal{E}_{calc}$ and attributed to turbulence (u_{turb}). Reference lines show typical zooplankton swimming speeds, as in (**f**).
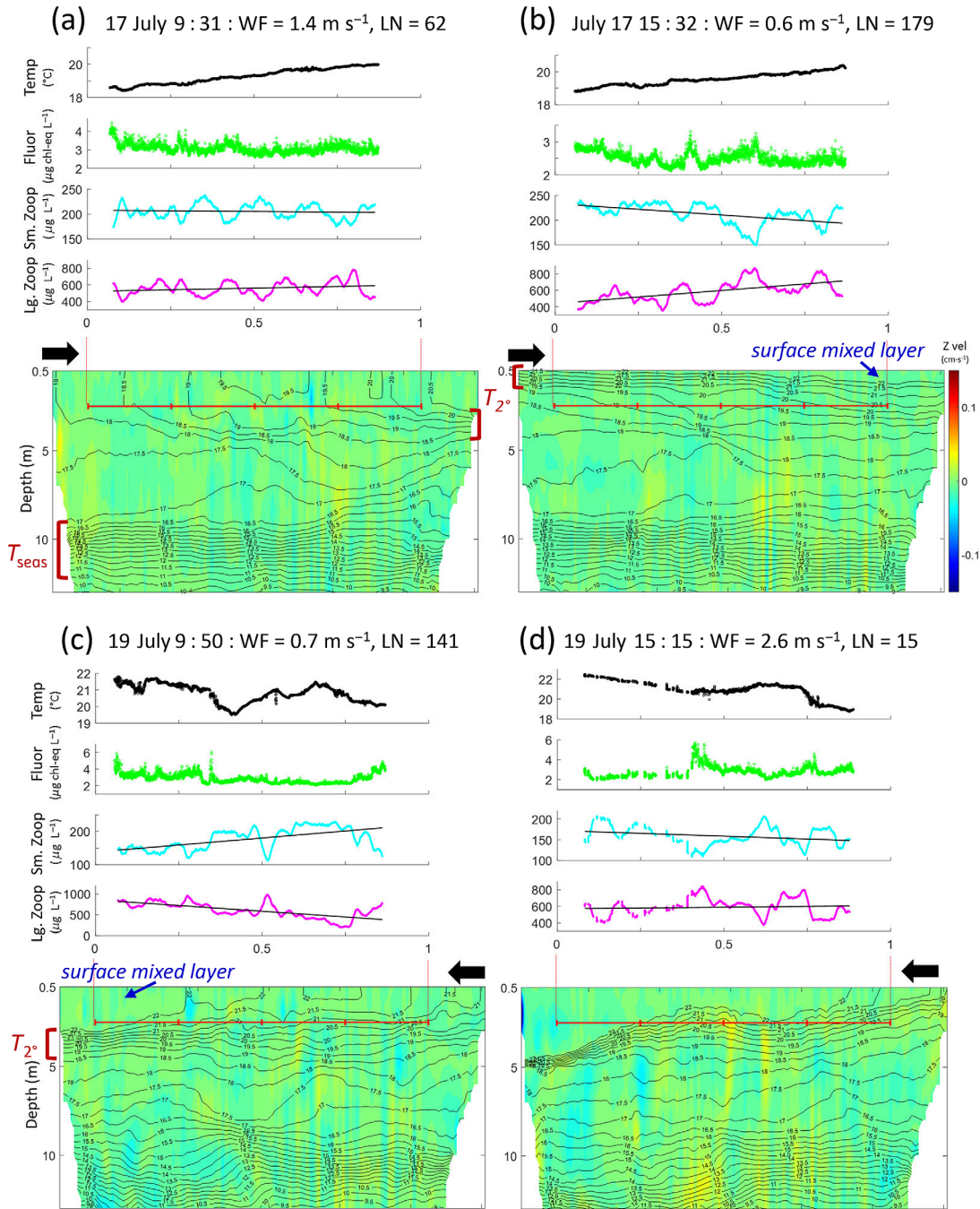
Fig. 4. OPC transects of temperature (Temp), fluorescence (Fluor), and small and large zooplankton biomass (Sm Zoop, Lg Zoop) shown with ELCOM-generated thermal stratification ($0.5°C$ isotherms) and vertical currents (Z vel, in cm s^{-1}, red upward, blue downward) in South Arm comparing calm and windy conditions. Transects are shown from west (left) to east (right), black arrows show wind direction. Horizontal red lines in ELCOM panels show standard OPC transect position (depth = 2.5 m; Fig. 2). Transect plots show individual Temp and Fluor measurements, zooplankton biomass filtered at ~ 100 m spatial scale (colored lines), and the basin wide linear change in biomass (straight black lines) used to calculate the RBI (Supporting Information Fig. S1). (**a,b**) Transects sampled over a calm 6-h period; (**c–d**) transects sampled over a 5.5-h period as easterly winds increased in speed; (**e–h**) two consecutive days with strong westerly winds in early July and mid-July. Date and time of sampling, wind force (WF, in m s^{-1}) and Lake Number (LN) averaged over T/4 h prior to sampling, are shown above each panel. The high LN value in panel e reflects low overnight winds before they strengthened again midday on 04 July (Supporting Information "Detailed time series" section). Note that biomass distributions of small and large zooplankton are out of phase under calm conditions (**a–d**, all X-corr = −0.89), mostly in phase under windy conditions (**e–g**, X-corr = +0.57 to + 0.65), but became decoupled on 14 July (**h**, X-corr = +0.02) after a long period of high winds. T_{seas}, $T_{2°}$, and surface mixed layer as in Fig. 1.
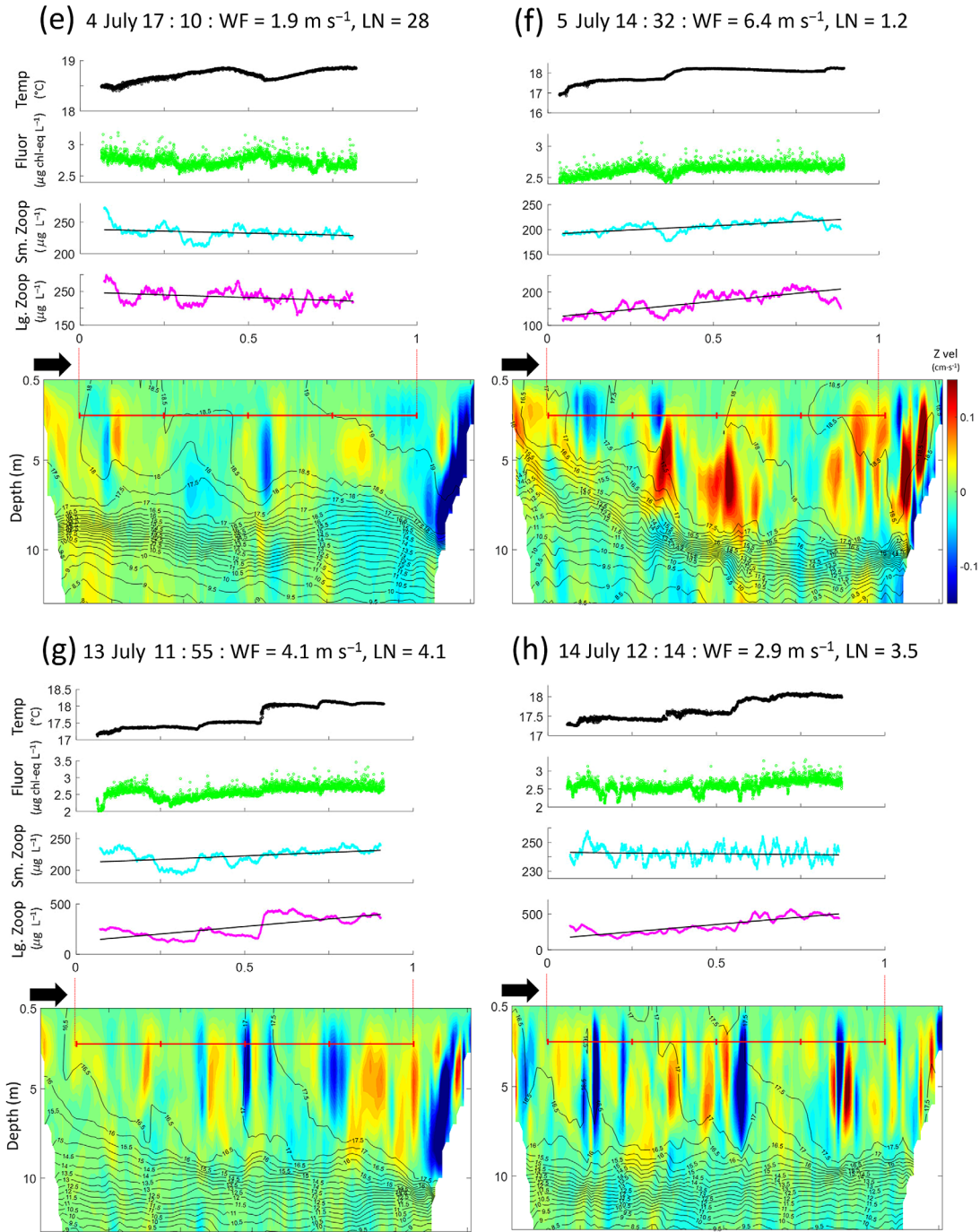
Fig. 4 (Continued)

forces of the upper epilimnion affect zooplankton distributions (Fig. 4; Supporting Information Fig. S3).

At the scale of the whole basin our expectation was that stronger winds would lead to higher near-surface plankton biomass at the downwind end of South Arm, especially in small zooplankton. As expected, we did find a positive relationship between the RBI of small zooplankton and LN, but no statistically significant relationship for large zooplankton (Table 2; Fig. 5a,b). However, the positive relationship detected in small zooplankton shows a lot of scatter in RBI on days with intermediate wind force (Fig. 5a). Small zooplankton were consistently more abundant downwind/upwind
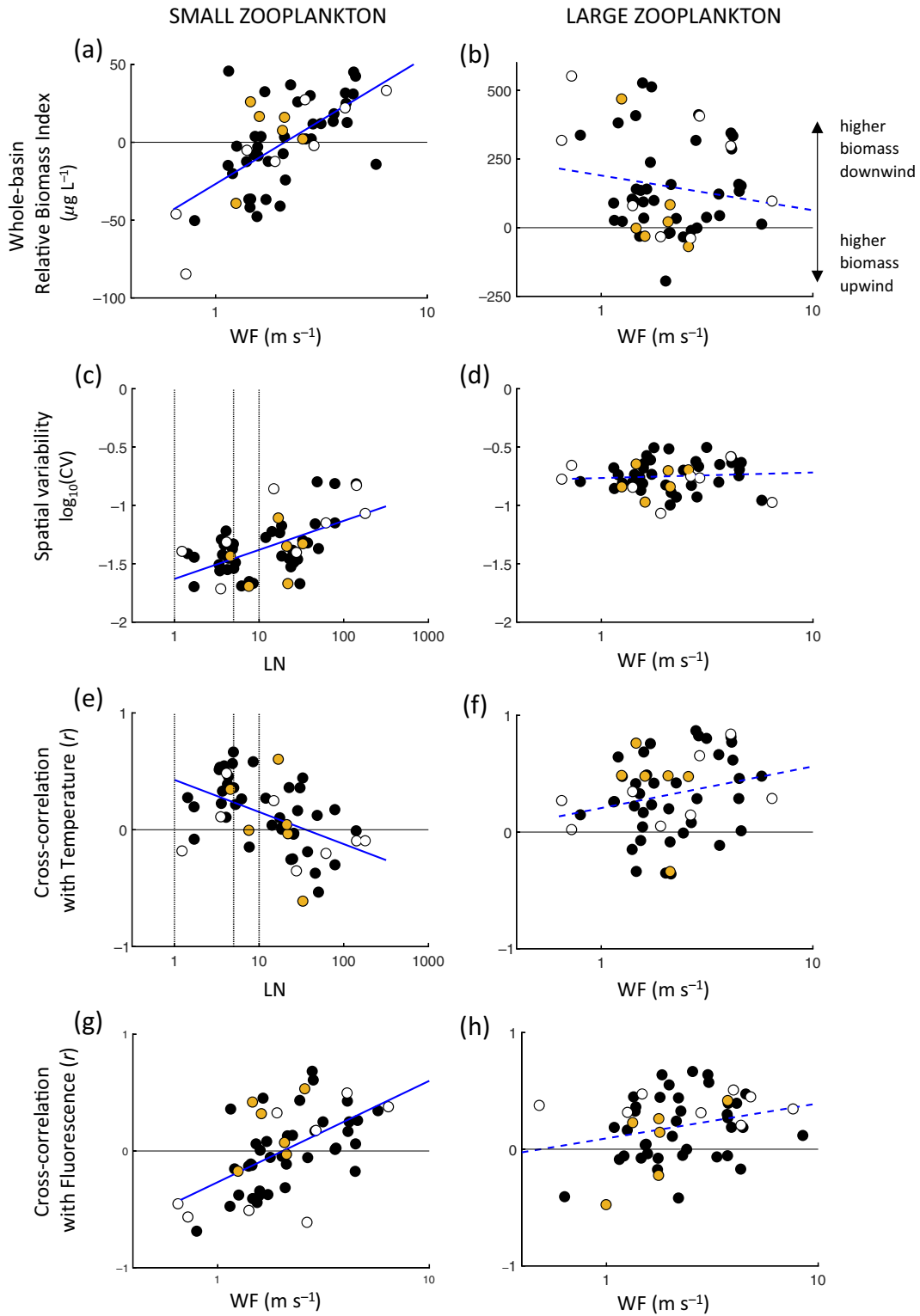
Fig. 5. Best relationships between different aspects of the distribution of small and large zooplankton and physical forces: (**a,b**) whole-basin RBI, with positive/negative RBI indicating higher/lower biomass downwind, (**c,d**) small-scale spatial variability (log$_{10}$ CV), and cross-correlation between zooplankton and water temperature (**e,f**) or fluorescence (**g,h**). WF is mean wind force and LN mean lake number both calculated over *T*/4 h prior to sampling except panel h calculated over prior 2 h. Open symbols are transects collected in July over a wide range of wind conditions, shown in Fig. 4; shaded orange symbols are transects collected during intermediate wind conditions from early to late stratification, shown in Supporting Information Fig. S3. Best-fit lines are shown (solid—*p* < 0.05; dotted—non-significant relationships; Table 2). Vertical reference lines in (**c,e**) are LN values of 1, 5, and 10.

following strong/weak winds but have more variable basin wide distributions following periods of moderate winds. Some of these deviations are likely due to transitional dynamics as discussed in the next section. In contrast, the biomass of large zooplankton was usually higher downwind relative to upwind or showed no trend across the lake basin (RBI ≥ 0; Fig. 5b), regardless of Wind Force or Lake Number ($p > 0.2$). Unlike small zooplankton only a few transects are below the horizontal line in Fig. 5b. These results suggest that large-bodied zooplankton respond to stratification and wind-driven hydrodynamics in a different way than smaller zooplankton.

At a fine spatial scale we hypothesized that the spatial variability, or patchiness, in zooplankton biomass would be greatest under calm stratified conditions but would gradually erode as turbulent mixing increased with strengthening winds. We found the expected relationship in small-bodied, but not large-bodied zooplankton (Table 2, Fig. 5d,e). The fine-scale spatial variability of small zooplankton (CV = 2–16%) was best related to Lake Number (Table 2). Small zooplankton showed low fine-scale spatial variability following very windy periods with LN < 10, high spatial variability during calm periods (LN > 50) and more variable CV under intermediate conditions (Fig. 5c). In contrast, large zooplankton consistently showed higher fine-scale variability (CV = 9–31%), regardless of WF or LN (Table 2; Fig. 5d). These results also suggest that large zooplankton respond to stratification and wind-driven hydrodynamics differently than small zooplankton.

Temperature and, to some extent, algal fluorescence can be used to trace the movement of water masses, so we tested whether the zooplankton biomass measured along individual transects was cross-correlated to either of these measurements, and whether these cross-correlations became stronger or weaker with increasing physical forces.

The cross-correlations between biomass and temperature or algal fluorescence were significantly related to both physical variables in small, but not in large zooplankton (Table 2; Fig. 5e–h). During calm periods small zooplankton biomass was negatively cross-correlated with temperature and fluorescence (suggesting greater biomass in colder, deeper strata) but became positively cross-correlated with both variables after high winds. In contrast, large zooplankton biomass was mostly positively cross-correlated with both temperature and fluorescence, but these cross-correlations were not statistically related to the physical forces ($p ≥ 0.05$, Table 2). These different relationships suggest that small and large zooplankton position themselves differently in the water column, especially during calm periods.

The strongest cross-correlations within transects were found between small and large zooplankton biomass, and the magnitude and direction of these cross-correlations were strongly related to both Wind Force and Lake Number (Table 2, Fig. 6). Small and large zooplankton biomass were negatively related to each other under calm conditions (low WF, high LN), but became positively related to each other
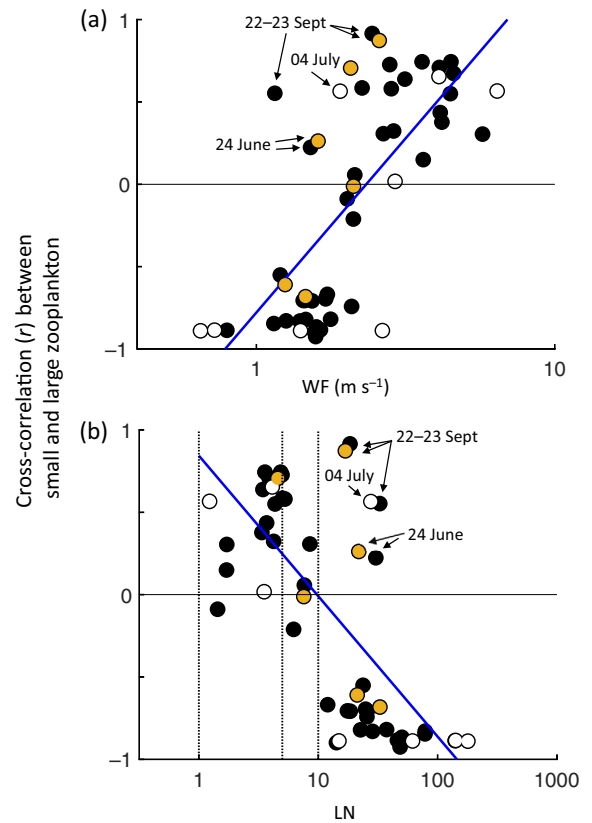

Fig. 6. Relationships between small and large zooplankton cross-correlation (*r* value) vs. (**a**) mean Wind Force (WF) and (**b**) geometric mean Lake Number (LN), both calculated over *T*/4 h prior to sampling (fitted linear regressions shown; statistics in Table 2). Vertical dashed reference lines and symbols as in Fig. 5. Arrows identify transects discussed in the text.

under windier conditions. These results also suggest that small and large zooplankton are positioned in different parts of the stratified water column during calm conditions but tend to get entrained together when strong winds homogenize the upper epilimnion and increase upwelling activity.

A few transects deviated from this relationship, with positive cross-correlations between small and large zooplankton despite relatively calm conditions (Fig. 6). Three of these exceptions occurred during fall (22–23 September) when strong convective cooling occurs (*w**, Fig. 3f) and the epilimnion only weakly stratifies during the day (< 1°C difference down to the seasonal thermocline; Supporting Information Figs. S3F, S8). The other three exceptions (24 June, 04 July) were morning samples or followed more extended periods of negative heat flux (Supporting Information Figs. S7, S5).

Zooplankton biomass in the upper water column

We present a subset of 14 transect samples along with ELCOM model outputs, which cover a range of wind conditions from early to late stratification, to help visualize the role of stratification and hydrodynamic forces on zooplankton

distribution. Samples in Fig. 4 and Supporting Information Fig. S3 are identified as open and orange symbols, respectively, in Figs. 5, 6.

The transects in Fig. 4a–d were sampled during calm to moderately windy periods when a secondary thermocline ($T_{2°}$) was present in the upper 5 m of the water column, well above the seasonal thermocline (T_{seas}). In the morning of 17 July, following a night of negative heat flux, $T_{2°}$ was located below our transect and moderate westerly winds produced upwelling of the $T_{2°}$ isotherms to the lake surface and displaced the (prior) surface layer (above 20.5°C isotherm) downwind (Fig. 4a; Supporting Information Fig. S4). The OPC transect did not extend into the displaced surface layer (Fig. 4a). Along this transect small zooplankton biomass was higher at the upwind end of the basin ($RBI_{SmZ} = -5 \, \mu g \, L^{-1}$) while large zooplankton biomass was higher downwind ($RBI_{LgZ} = +80 \, \mu g \, L^{-1}$), and their distributions were strongly out-of-phase along the whole transect (X-corr $= -0.89$). These observations suggest that small and large zooplankton are concentrated in different $T_{2°}$ strata, with small zooplankton positioned in deeper, cooler strata than large zooplankton. Similar conditions on 10 July later in the day (Supporting Information Fig. S3E), resulted in much larger basin wide differences in zooplankton biomass ($RBI_{SmZ} = -39 \, \mu g \, L^{-1}$, $RBI_{LgZ} = +469 \, \mu g \, L^{-1}$).

Weakening winds and sunny conditions resulted in strong stratification ($\sim 3°C$) developing right below the lake surface in the afternoon of July 17, above our transect (Fig. 4b). Mild westerly winds pushed the thin surface mixed layer downwind and tilted the subsurface thermocline down to our transect. The OPC transect sampled across several isotherms (18.5°–20°) but remained below the displaced surface mixed layer. Zooplankton distribution was similar to the morning sample, but the basin wide biomass patterns were stronger ($RBI_{SmZ} = -46 \, \mu g \, L^{-1}$, $RBI_{LgZ} = +318 \, \mu g \, L^{-1}$) and the two size classes were strongly out of phase with each other (X-corr $= -0.89$; Fig. 4b). Mild westerly winds were also blowing on a surface stratified layer in the afternoon of 08 July (Supporting Information Fig. S3D), but this time our transect sampled below this surface stratified layer across the remnant well-mixed epilimnetic water mass that was displaced downwind over the previous four stormy days (note increased winds and low L_N in the previous 4 d; Supporting Information Fig. S5). The distribution of small and large zooplankton in the afternoon of 08 July was also out-of-phase (X-corr $= -0.68$), but this time we observed higher biomass of small zooplankton downwind ($RBI_{SmZ} = +26 \, \mu g \, L^{-1}$) in the upper portion of the displaced epilimnion and no basin wide difference in large zooplankton biomass ($RBI_{LgZ} = -2 \, \mu g \, L^{-1}$). The transitional conditions on 08 July resulted in one of the largest positive deviations from the overall relationship between small zooplankton RBI and wind force (highest orange circle in Fig. 5a) and is in the lower range of large zooplankton RBI (Fig. 5b).

Five transects were sampled over a 5.5-h period on 19 July (first and last shown in Fig. 4c,d) as the easterly winds built from mild to moderate speeds (1.5 to 4–5 m s^{-1}; Supporting Information Fig. S4). $T_{2°}$ was located just below our transect but progressively became more tilted and more energized (notice $T_{2°}$ internal wave in Fig. 4d). The tilted $T_{2°}$ produced the observed downwind increase in water temperature along each transect. All 19 July transects showed clear out-of-phase distribution of small and large zooplankton (X-corr $= -0.85$ to -0.92; e.g., Fig. 4c,d). The first four 19 July transects sampled within $T_{2°}$ all show lower biomass of small zooplankton but higher biomass of large zooplankton downwind compared to upwind ($RBI_{SmZ} = -83$ to $-3 \, \mu g \, L^{-1}$, $RBI_{LgZ} = +552$ to $+90 \, \mu g \, L^{-1}$). These basin wide differences in zooplankton biomass dampened from morning to early afternoon (i.e., both RBI tend to zero). The last transect traversed from the (tilted) secondary thermocline at the upwind end of the basin into the displaced upper mixed layer downwind (Fig. 4d), and this transect showed reversed basin wide distributions compared to earlier 19 July transects, for both small and large zooplankton ($RBI_{SmZ} = +27 \, \mu g \, L^{-1}$, $RBI_{LgZ} = -39 \, \mu g \, L^{-1}$). These progressive changes in RBI over a period of 5.5 h follow the overall relationship between RBI_{SmZ} and wind force (Fig. 5a) and highlight the dynamic nature of water column structure and of zooplankton distribution.

All transects on these calm to moderately windy days were sampling a stratified portion of the epilimnion and showed multiple fluorescence peaks, high small-scale zooplankton variability ($CV_{SmZ} = 0.07-0.16$, $CV_{LgZ} = 0.14-0.22$) and clear out-of-phase distribution of small and large zooplankton (Fig. 4a, d). This suggests that small and large zooplankton position themselves at different depths relative to the isotherms and are sampled as the isotherms oscillate up and down across our constant depth transect.

The transects shown in the next four panels of Fig. 4e–h were sampled following some of the windiest days (Supporting Information Figs. S4, S5) and show partial upwellings from the upper portion of the seasonal thermocline. These transects cross from distinct metalimnetic water masses into the surface mixed layer that was blown downwind. This creates clear stepwise increases in water temperature toward the downwind end of each transect. In several cases similar stepwise patterns can be seen in large zooplankton biomass (Fig. 4f–h). On these windy days, the distributions of small and large zooplankton are usually in phase with each other (X-corr $= +0.57$ to $+0.65$) and their basin wide distribution is similar (Fig. 4e–g). However, on 14 July the distribution of small zooplankton became more homogeneous, at both fine ($CV_{SmZ} = 0.02$) and basin wide ($RBI_{SmZ} = -2$) spatial scales, and decoupled from large zooplankton (X-corr $= 0.02$; Fig. 4h). Low spatial variability of small zooplankton and decoupling from large zooplankton were also observed on 06 June ($CV_{SmZ} = 0.02$, X-corr $= -0.01$; Supporting Information Fig. S3A) and on 24 June ($CV_{SmZ} = 0.02$, X-corr $= +0.26$; Supporting Information Fig. S3C) when the upper water column was mixed by winds and thermal convection (Supporting Information Figs. S6, S7).

Fluorescence also tends to be less spatially variable on windy than on calm days (note difference in *Y*-axis scale in Fig. 4a–d), with some clear fluorescence troughs on days with stronger vertical currents (Fig. 4f,h).

Grouped analysis of zooplankton spatial responses

The regression analyses we used to assess relationships between physical variables and spatial patterns of zooplankton biomass implicitly assume the underlying physical processes to be continuous. However, stratification of the upper water column is not continuous because a secondary thermocline may or may not be present. To address this issue, we grouped our observations into stratified, partially mixed, and mixed conditions based on the thermal structure of the water column at the time of sampling and compared the mean values of each measure of zooplankton distribution among these conditions (Supporting Information "Grouped analysis" section). This grouped analysis confirms the results from the regression analysis with continuous wind forcing variables presented above (Supporting Information Fig. S9).

Discussion

Physical forces in the upper water column are complex and dynamic, making it difficult to follow the distribution of planktonic organisms. Improvements in our understanding of wind-driven hydrodynamic forces in lakes and of behavior in different groups of planktonic organisms can help us predict changes in plankton distribution and in the dynamics of trophic interactions at the base of lake food webs.

Do zooplankton accumulate downwind on windy days?

Positively buoyant organisms have long been observed to aggregate along downwind shores (e.g., cyanobacterial blooms; Small 1963; Malone and McQueen 1983). Wind-generated currents are strongest at the surface and can result in rapid transport of surface water and plankton downwind. Depth of the surface mixed layer will determine how much surface water is displaced downwind. This varies with wind strength, convective cooling and the strength of stratification of the upper water column.

Our hydrodynamic model shows surface mixed layers getting displaced downwind that range from very shallow layers (< 0.5 m) on calm sunny days all the way to the full epilimnion being pushed downwind by partial upwelling of the seasonal thermocline on very windy days. When winds were light we observed that large zooplankton were more abundant downwind, in warmer surface water masses displaced for a few hours to days depending on the winds. By contrast small zooplankton, were more abundant upwind where cooler (deeper) strata moved closer to the lake surface due to a slight tilt of the secondary thermocline. These distinct spatial patterns in large and small zooplankton arise because under light winds zooplankton of all sizes can position themselves at different depths in the stratified upper water column. Others have

found that freshwater and marine zooplankton can select and maintain their depth in the water column in areas where prey and mates are abundant or to reduce predation (Ragotzkie and Bryson 1953; True et al. 2015). Near-surface stratification is common in Lake Opeongo, where despite the use of low-resolution thermistors we detected stratification in the upper 2 m of the epilimnion, from at least one of the thermistor strings, 36% of the time between 01 June and 23 September.

By contrast when winds are strong our results show that both large- and small-bodied zooplankton biomasses are relatively greater in the displaced epilimnion at the downwind end of the basin. Part of this basin wide pattern is due to the upwelling of zooplankton-depleted metalimnetic water at the upwind end of the basin. But Cyr and Sprules (2022) also showed that on windy days the biomass of small zooplankton in the displaced (downwind) water mass was always higher than in the surface water during calm periods (i.e., in its original position). This suggests that even small zooplankton play an active role in positioning themselves in the upper epilimnion on windy days.

Rapid basin wide displacement of zooplankton could also occur in strongly stratified portions of the water column where vertical mode 2 (V2H1) waves develop and create basin wide currents by compressing and expanding the metalimnion (fig. 2c in Boegman 2009). This phenomenon affects the basin wide distribution of *Planktothrix* (Cuypers et al. 2011) and should have a similar effect on any planktonic organisms. Our hydrodynamic model suggests V2 dynamics are common in Lake Opeongo, both in the seasonal and secondary thermoclines.

Does zooplankton patchiness decrease with increasing winds?

Zooplankton can position themselves in the water column when winds are light, and this would create patchiness at small spatial scales (Johnson et al. 2007). Phytoplankton have also been shown to aggregate under calm and moderately windy conditions, but their vertical and horizontal patchiness both disappear when physical forces overwhelm their buoyancy during windy periods (Small 1963; George and Edwards 1976; Reynolds et al. 1987) and during nighttime convective cooling (Serra et al. 2007). The threshold at which zooplankton patchiness disappears is expected to vary as a function of their size-dependent swimming abilities.

For small zooplankton, we found clear relationships between fine-scale spatial variability and physical forcing indicating that mixing erodes the spatial patterns that existed under calm conditions. Large zooplankton were consistently more spatially variable than small ones, and their spatial variability was not affected by wind conditions. Planktivory is intense in Lake Opeongo (Milne et al. 2005), and large zooplankton are more vulnerable to visual predators than small zooplankton. High spatial variability of large offshore zooplankton could result from predation by swarming cisco

(Milne et al. 2005) or from swarming behavior of the zooplankton to reduce encounter and per capita mortality from visual predators (Tessier 1983). This difference in susceptibility to physical mixing in the water column is consistent with large zooplankton being able to resist a broader range of current speeds than small zooplankton.

Do winds change spatial relationships in plankton communities?

The most striking fine-scale spatial pattern in our data is a shift from strong negative cross-correlations between the two zooplankton size classes under calm conditions to strong positive cross-correlations as the wind increases. This means that the two groups are patchy and almost perfectly out of phase during very calm conditions but become more synchronous with stronger winds.

During calm to moderately windy conditions some of the zooplankton patchiness also coincides with peaks in fluorescence. This is likely due to persistent vertical movement of isotherms in the stratified epilimnion as revealed by the hydrodynamic model. On calm days small zooplankton are usually negatively cross-correlated with water temperature while large zooplankton are positively cross-correlated with temperature. This suggests that small and large zooplankton aggregate along different isotherms and is thus entrained past the OPC sensors at different times (Pernica et al. 2013). The negative cross-correlation between small and large zooplankton during calm periods could also be due to direct consumption of small zooplankton by larger predatory species, a pattern that would disappear with increased mixing during windier periods.

As the winds strengthen, small and large zooplankton may become overwhelmed by mixing forces and become entrained together. Our hydrodynamic model suggests that deep vertical mixing cells develop in the epilimnion under strong winds and troughs in the fluorescence transects are consistent with this type of mixing. Such vertical mixing cells are difficult to detect without fine-scale horizontal data but are likely common (Austin 2019; Bouffard and Wüest 2019).

During the windiest periods we observed periodic sharp increases in water temperature from the upwind to the downwind end of the basin. These patterns are due to these transects crossing progressively warmer water masses, from upwelled (cold) metalimnetic water at the upwind end of the basin to displaced (warm) surface water at the downwind end of the basin. There is also a progressive increase in zooplankton biomass reflecting increasing concentrations from metalimnetic to epilimnetic strata. Interestingly, on 13 July there are also sharp increases in large zooplankton biomass along the transect suggesting isolated water masses. A slight decline in large zooplankton biomass between sharp increases likely reflects the circulation in these upwelled water masses (Mortimer 1952). There was a progressive loss of these sharp transitions in water temperature, but especially in

zooplankton biomass, as winds weakened over the following 24 h. This is consistent with "edge leakage" of upwelled water masses, which is expected from wind shear-flow dispersion at the lake surface (Monismith and MacIntyre 2009). After a cold windy night (air temperature < 15°C), the distinction in water temperature between the metalimnetic water masses was still evident but was mostly lost from the large zooplankton data. Nighttime convection likely altered the pattern of circulation within the upwelled water masses, and the distribution of plankton. The distribution of small zooplankton showed weaker differences among water masses but similar homogenization over time.

Implications for lake food webs

The relation between physical forces in lakes and zooplankton body size raises the question of how wind-induced hydrodynamics could affect trophic interactions. Effects will of course vary among lakes, but our results for Lake Opeongo can be considered representative of systems that have an open fetch oriented generally in the direction of prevailing winds.

At the basin scale, we found that downwind concentrations of zooplankton were higher than upwind concentrations, particularly when strong winds displaced the whole epilimnion downwind. Water masses that get close to shore during periods of strong up/downwelling could receive nutrient subsidies from the sediments that alter nutrient limitation in phytoplankton (Cyr and Coman 2012) and possibly affect the efficiency of energy transfer to herbivorous zooplankton. Higher in the food web, planktivorous fish have been shown to aggregate at the downwind end of South Arm on windy days, presumably taking advantage of higher prey concentrations (de Kerckhove et al. 2015). Smallmouth bass nesting sites in South Arm are heavily concentrated along the downwind shore (Rejwan et al. 1997), and bass larvae at these sites reach a larger size than upwind (Kaevats et al. 2005). For more sedentary organisms that use zooplankton as prey, downwind habitats should be of higher quality, especially since they tend, on average, to be warmer than upwind sites (Finlay et al. 2001). The impact of plankton subsidies on nearshore communities in lakes is generally ignored and requires more attention (Cyr and Sprules 2022).

Changes in the fine-scale patchiness of small zooplankton under different wind conditions could also affect the efficiency of trophic transfers in planktonic communities. Patches of small zooplankton could attract predatory copepods such as *Epischura lacustris* and *Mesocyclops edax* much as thin algal layers have been shown to attract heterotrophic dinoflagellates (Menden-Deuer and Grünbaum 2006). If spatial patchiness increases feeding efficiency (Reid and Sprules 2018), our results suggest that the relative role of small and large zooplankton in planktonic food webs may change as the winds become stronger.

Near-surface turbulence on windy days could affect feeding of both grazing and predatory zooplankton (Saiz and

Kiorboe 1995; Visser and Stips 2002). The upper epilimnion in Lake Opeongo tends to be thermally stratified when winds are light to moderate. Turbulence is expected to be low under these conditions and it is likely that feeding by both predatory and grazing zooplankton would be enhanced. The role of turbulence on zooplankton feeding deserves more attention. Our current understanding is limited to large marine zooplankton studied in laboratory experiments where turbulence is generally much higher than in nature (Franks et al. 2022).

Conclusions

In summary, our study provides evidence that wind-driven physical processes affect the spatial ecology of zooplankton in the epilimnion of a typical Canadian Shield lake. The most important result is that the response of zooplankton to these physical forces is strongly dependent on an interaction between their body size and the spatial scale and intensity of the wind-generated physical forces. We have discussed implications of these results for food web interaction in lakes; however, there is a dearth of direct observations in lakes on feeding interactions within planktonic communities, and between planktonic and nearshore benthic communities under varying hydrodynamic forces and these would be important research initiatives in future.

References

Austin, J. A. 2019. Observations of radiatively driven convection in a deep lake. Limnol. Oceanogr. **64**: 2152–2160. doi:10.1002/lno.11175

Boegman, L. 2009. Currents in stratified water bodies 2: Internal waves, p. 539–558. *In* G. E. Likens [ed.], Encyclopedia of inland waters. Academic Press.

Bouffard, D., and A. Wüest. 2019. Convection in lakes. Annu. Rev. Fluid Mech. **51**: 189–215. doi:10.1146/annurev-fluid-010518-040506

Cuypers, Y., B. Vinçon-Leite, A. Groleau, B. Tassin, and J. F. Humbert. 2011. Impact of internal waves on the spatial distribution of *Planktothrix rubescens* (cyanobacteria) in an alpine lake. ISME J. **5**: 580–589. doi:10.1038/ismej.2010.154

Cyr, H. 2016. Wind-driven thermocline movements affect the colonisation and growth of *Achnanthidium minutissimum*, a ubiquitous benthic diatom in lakes. Freshw. Biol. **61**: 1655–1670. doi:10.1111/fwb.12806

Cyr, H. 2017. Winds and the distribution of nearshore phytoplankton in a stratified lake. Water Res. **122**: 114–127. doi:10.1016/j.watres.2017.05.066

Cyr, H., and M. A. Coman. 2012. Wind-driven physical processes and sediment characteristics affect the distribution and nutrient limitation of nearshore phytoplankton in a stratified. Limnol. Oceanogr. Fluids Environ. **2**: 93–108. doi:10.1215/21573689-1964968

Cyr, H., and W. G. Sprules. 2022. The wind-driven distribution of nearshore zooplankton in a stratified lake varies with their body size. Freshwat. Biol. **67**: 991–1004.

de Kerckhove, D. T., E. A. Blukacz-Richards, B. J. Shuter, L. Cruz-Font, and P. A. Abrams. 2015. Wind on lakes brings predator and prey together in the pelagic zone. Can. J. Fish. Aquat. Sci. **72**: 1652–1662. doi:10.1139/cjfas-2015-0119

Denman, K. L., and A. E. Gargett. 1983. Time and space scales of vertical mixing and advection of phytoplankton in the upper ocean. Limnol. Oceanogr. **28**: 801–815.

Finlay, K., B. E. Beisner, and A. J. D. Barnett. 2007. The use of the laser optical plankton counter to measure zooplankton size, abundance, and biomass in small freshwater lakes. Limnol. Oceanogr. Methods **5**: 41–49. doi:10.4319/lom.2007.5.41

Finlay, K. P., H. Cyr, and B. J. Shuter. 2001. Spatial and temporal variability in water temperatures in the littoral zone of a multibasin lake. Can. J. Fish. Aquat. Sci. **58**: 609–619. doi:10.1139/cjfas-58-3-609

Franks, P. J. S., B. G. Inman, J. A. MacKinnon, M. H. Alford, and A. F. Waterhouse. 2022. Oceanic turbulence from a planktonic perspective. Limnol. Oceanogr. **67**: 348–363. doi:10.1002/lno.11996

George, D. G., and R. W. Edwards. 1976. The effect of wind on the distribution of chlorophyll a and crustacean plankton in a shallow eutrophic reservoir. J. Appl. Ecol. **13**: 667–690.

George, D. G., and S. I. Heaney. 1978. Factors influencing the spatial distribution of phytoplankton in a small productive lake. J. Ecol. **66**: 133–155.

Hodges, B., and C. Dallimore. 2014. Estuary, Lake and Coastal Ocean Model: ELCOM. v2.2 science manual. Centre for Water Research, Univ. of Western Australia.

Holland, J. D., D. G. Bert, and L. Fahrig. 2004. Determining the spatial scale of species' response to habitat. Bioscience **54**: 227–233.

Imberger, J. 1985. The diurnal mixed layer. Limnol. Oceanogr. **30**: 737–770. doi:10.4319/lo.1985.30.4.0737

Johnson, C. R., W. J. O'Brien, and S. MacIntyre. 2007. Vertical and temporal distribution of two copepod species, *Cyclops scutifer* and *Diaptomus pribilofensis*, in 24 h arctic daylight. J. Plankton Res. **29**: 275–289. doi:10.1093/plankt/fbm014

Kaevats, L., W. G. Sprules, and B. J. Shuter. 2005. Effects of wind-induced spatial variation in water temperature and zooplankton concentration on the growth of young-of-the-year smallmouth bass, *Micropterus dolomieu*. Environ. Biol. Fishes **74**: 273–281. doi:10.1007/s10641-005-4419-2

Malone, B. J., and D. J. McQueen. 1983. Horizontal patchiness in zooplankton populations in two Ontario kettle lakes. Hydrobiologia **99**: 101–124. doi:10.1007/BF00015039

Menden-Deuer, S., and D. Grünbaum. 2006. Individual foraging behaviors and population distributions of a planktonic predator aggregating to phytoplankton thin layers. Limnol. Oceanogr. **51**: 109–116. doi:10.4319/lo.2006.51.1.0109

Menza, C. W. 2003. Effects of wind on horizontal zooplankton spatial patterns in Lake Opeongo, Ontario, Canada. MSc thesis. Univ. of Toronto.

Milne, S. W., B. J. Shuter, and W. G. Sprules. 2005. The schooling and foraging ecology of lake herring (*Coregonus artedi*) in Lake Opeongo, Ontario, Canada. Can. J. Fish. Aquat. Sci **62**: 1210–1218.

Monismith, S. G., and S. MacIntyre. 2009. The surface mixed layer in lakes and reservoirs, p. 636–650. *In* G. E. Likens [ed.], Encyclopedia of inland waters. Academic Press.

Mortimer, C. H. 1952. Water movements in lakes during summer stratification; evidence from the distribution of temperature in Windermere. Philos. Trans. R. Soc. Lond. B Biol. Sci. **236**: 355–398. doi:10.1098/rstb.1952.0005

Pernica, P., M. G. Wells, and W. G. Sprules. 2013. Internal waves and mixing in the epilimnion of a lake affects spatial patterns of zooplankton in a body-size dependent manner. Limnol. Oceanogr. Fluids Environ. **3**: 279–294. doi:10.1215/21573689-2409149

Prairie, J. C., K. R. Sutherland, K. J. Nickols, and A. M. Kaltenberg. 2012. Biophysical interactions in the plankton: A cross-scale review. Limnol. Oceanogr. Fluids Environ. **2**: 121–145. doi:10.1215/21573689-1964713

Ragotzkie, R. A., and R. A. Bryson. 1953. Correlation of currents with the distribution of adult *Daphnia* in Lake Mendota. J. Mar. Res. **12**: 157–172.

Read, J. S., D. P. Hamilton, I. D. Jones, K. Muraoka, L. A. Winslow, R. Kroiss, C. H. Wu, and E. Gaiser. 2011. Derivation of lake mixing and stratification indices from high-resolution lake buoy data. Environ. Model. Software **26**: 1325–1336. doi:10.1016/j.envsoft.2011.05.006

Reid, A. H., and W. G. Sprules. 2018. A comprehensive evaluation of *Daphnia pulex* foraging energetics and the influence of spatially heterogeneous food. Inland Waters **8**: 50–59. doi:10.1080/20442041.2018.1427950

Rejwan, C., B. J. Shuter, M. S. Ridgway, and N. C. Collins. 1997. Spatial and temporal distributions of smallmouth bass (*Micropterus dolomieu*) nests in Lake Opeongo. Ontario Can. J. Fish. Aquat. Sci. **54**: 2007–2013. doi:10.1139/cjfas-54-9-2007

Reynolds, C. S., R. L. Oliver, and A. E. Walsby. 1987. Cyanobacterial dominance: The role of buoyancy regulation in dynamic lake environments. New Zealand J. Mar. Freshw. Res. **21**: 379–390. doi:10.1080/00288330.1987.9516234

Saiz, E., and T. Kiorboe. 1995. Predatory and suspension feeding of the copepod *Acartia tonsa* in turbulent environments. Mar. Ecol. Prog. Ser. **122**: 147–158. doi:10.3354/meps122147

Serra, T., J. Vidal, X. Casamitjana, M. Soler, and J. Colomer. 2007. The role of surface vertical mixing in phytoplankton distribution in a stratified reservoir. Limnol. Oceanogr. **52**: 620–634. doi:10.4319/lo.2007.52.2.0620

Small, L. F. 1963. Effect of wind on the distribution of chlorophyll *a* in clear Lake. Iowa Limnol. Oceanogr. **8**: 426–432.

Sprules, W. G., E. H. Jin, A. W. Herman, and J. D. Stockwell. 1998. Calibration of an optical plankton counter for use in fresh water. Limnol. Oceanogr. **43**: 726–733. doi:10.4319/lo.1998.43.4.0726

Stevens, C., and J. Imberger. 1996. The initial response of a stratified lake to a surface shear stress. J. Fluid Mech. **312**: 39–66. doi:10.1017/S0022112096001917

Tessier, A. J. 1983. Coherence and horizontal movements of patches of *Holopedium gibberus* (Cladocera). Oecologia **60**: 71–75.

True, A. C., D. R. Webster, and M. J. Weissburg. 2015. Patchiness and depth-keeping of copepods in response to simulated frontal flows. Mar. Ecol. Prog. Ser. **539**: 65–76.

Verhagen, J. H. G. 1994. Modeling phytoplankton patchiness under the influence of wind-driven currents in lakes. Limnol. Oceanogr. **39**: 1551–1565. doi:10.4319/lo.1994.39.7.1551

Visser, A. W., and A. Stips. 2002. Turbulence and zooplankton production: Insights from PROVESS. J. Sea Res. **47**: 317–329. doi:10.1016/S1385-1101(02)00120-X

Wüest, A., and A. Lorke. 2003. Small-scale hydrodynamics in lakes. Annu. Rev. Fluid Mech. **35**: 373–412. doi:10.1146/annurev.fluid.35.101101.161220

Conflict of Interest

None declared.